ALEPH 2001-019
CONF 2001-016
February 20, 2001
Revised July 2, 2001

PRELIMINARY

Fermion Pair Production in e^+e^- Collisions at High Energy and Limits on Physics beyond the Standard Model

The ALEPH Collaboration

Contact person: M.N. Minard (marie-noelle.minard@cern.ch)

Abstract

Preliminary results on cross sections and forward-backward asymmetries from hadronic and leptonic events produced in e^+e^-collisions at centre-of-mass energies above 203 GeV are summarized, together with R_b and asymmetry measurements in the quark sector from data taken at 189 to 202 GeV. Results for e^+e^-, $\mu^+\mu^-$, $\tau^+\tau^-$, $q\bar{q}$ and $b\bar{b}$ production show no significant deviation from Standard Model predictions. These results combined with those at lower energies lead to more stringent constraints upon physics beyond the Standard Model such as four-fermion contact interactions, leptoquarks, R-parity violating sneutrinos and TeV scale quantum gravity.

Contributed paper for LP01 and EPS HEP 2001

1 Introduction

Measurements of cross-sections for the production of lepton and quark pairs in e^+e^- collisions at LEP are presented. For μ and τ pair production, differential cross-sections are also given and forward-backward asymmetries are extracted. The data used in this analysis were collected with the ALEPH detector during the year 2000 and are split into two energy bins, the highest energy point corresponding to the average over energies above 205.5 GeV, the highest energies reached at LEP. Table 1 summarizes the recorded luminosities for the two average energies, corresponding to a total integrated luminosity of $215.6 \pm 0.3(stat) \pm 1.0(syst)$ pb^{-1}. The analysis of the data follows closely the procedures described in [1] and [2].

In addition, new results from data taken in previous years are presented. The ratio R_b of the $b\bar{b}$ cross-section to the $q\bar{q}$ cross-section, the forward-backward asymmetry for b quarks A^b_{FB} and the forward-backward charge asymmetry for light quarks Q^{udsc}_{FB} are determined for centre of mass energies in the range of 192 to 202 GeV. Finally, the asymmetry for c quarks A^c_{FB} is given for a centre-of-mass energy of 189 GeV.

The inclusion of the high energy data improves in many cases limits upon extensions to the Standard Model (SM) with respect to previous ALEPH constraints [2] and [3].

Table 1: Luminosities for the different energies used in the present analysis.

E_{cm} (GeV)	Luminosity(pb^{-1})
204.97	81.288 ± 0.15(stat) ± 0.3(syst)
206.69	134.34 ± 0.19(stat) ± 0.5(syst)

2 Fermion Pair Production

Cross-sections are determined for two $\sqrt{s'}$ ranges detailed below. The variable $\sqrt{s'}$ is defined as the mass of the outgoing lepton pair for leptonic final states, whilst for hadronic final states $\sqrt{s'}$ is defined as the mass of the Z/γ^* propagator. The variable $\sqrt{s}$ is the centre-of-mass energy.

Cross-sections of fermion pair production are given for:

- inclusive production, i.e. including hard ISR with a loose s' cut ($\sqrt{s'/s} > 0.1$).
- exclusive production for which radiative returns to the Z resonance are removed by a tight s' cut ($\sqrt{s'/s} > 0.9$). In this case the angular range of the final state fermions is restricted to $|\cos\theta| < 0.95$ in order to be less sensitive to the effects of ISR/FSR interference.
- For the e^+e^- channel, because of the dominance of the t-channel exchange contribution, the cross sections are given for $\sqrt{s'/s} > 0.9$ only and for two angular ranges in the e^+e^- center of mass system : $|\cos\theta^*| < 0.9$ and $-0.9 < \cos\theta^* < 0.7$.

2.1 Di-fermion production above 203 GeV

The selection efficiencies and expected background contributions are summarized in Table 2. For the exclusive hadronic channel, efficiencies were calculated using KORALZ. They were checked with the KK2f Monte-Carlo which includes the latest version of DIZET for the box diagramm calculation and the EEX3 extension [4]. The discrepancy of 1% on the efficiencies observed between these generators is taken into account in the systematic uncertainty.

Table 2: Selection efficiencies and backgrounds with their statistical errors. For e^+e^- production, the efficiency is calculated for (1) $-0.9 < \cos\theta^* < 0.9$ and (2) $-0.9 < \cos\theta^* < 0.7$.

$\sqrt{s'/s}$ cut	E_{cm} (GeV)	Event type	Efficiency %	Background %
0.1	204.9	$q\bar{q}$	82.2 ± 0.2	24.6 ± 0.3
		$\mu^+\mu^-$	73.2 ± 0.2	12.3 ± 2.1
		$\tau^+\tau^-$	41.1 ± 0.2	19.9 ± 1.6
	206.7	$q\bar{q}$	81.9 ± 0.2	24.9 ± 0.3
		$\mu^+\mu^-$	72.9 ± 0.2	11.4 ± 2.0
		$\tau^+\tau^-$	41.3 ± 0.2	17.6 ± 2.0
0.9	204.9	$q\bar{q}$	85.7 ± 1.0	9.6 ± 0.1
		$\mu^+\mu^-$	96.1 ± 0.2	6.9 ± 1.0
		$\tau^+\tau^-$	63.9 ± 0.4	21.5 ± 2.0
		$e^+e^-(1\ )$	81.3 ± 0.4	11.0 ± 0.8
		$e^+e^-(2\ )$	93.4 ± 0.4	13.0 ± 1.0
	206.7	$q\bar{q}$	86.7 ± 1.0	9.7 ± 0.1
		$\mu^+\mu^-$	95.9 ± 0.2	5.3 ± 1.0
		$\tau^+\tau^-$	64.1 ± 0.4	19.2 ± 2.0
		$e^+e^-(1\ )$	81.7 ± 0.3	11.0 ± 0.3
		$e^+e^-(2\ )$	94.4 ± 0.4	12.6 ± 0.7

The measured cross sections are given in Table 3 and are compared to Standard Model predictions from ZFITTER (v6.30) [5] including ISR/FSR interference for $q\bar{q}$, $\mu^+\mu^-$, $\tau^+\tau^-$ and from the event generator BHWIDE [6] for e^+e^-. They are shown in Fig. 1 together with the ALEPH measurements at lower centre-of-mass energies [1] [2] [3] . Within the current uncertainties these measurements are in agreement with the Standard Model predictions.

For μ pair and τ pair events satisfying $\sqrt{s'/s} > 0.9$, the forward-backward asymmetries A^{μ}_{FB} and A^{τ}_{FB} are measured. They are obtained by counting the number of events for which the negatively charged lepton is in the forward or backward hemisphere, within the nominal angular range of $|\cos\theta| < 0.95$. The numerical results are given in Table 4 together with the Standard Model predictions. Fig. 2 displays all ALEPH asymmetries measurements([1], [2] and [3]) and compares them with the Standard Model expectation.

In order to combine data from all four LEP collaborations, the differential cross sections $d\sigma/dcos\theta$ of μ pair and τ pair production are measured for $\sqrt{s'/s} > 0.85$. These

Table 3: Preliminary cross sections for all recorded energies, together with their statistical and systematic errors. The exclusive processes are defined in the angular range $|\cos\theta| < 0.95$. For e^+e^-production, the cross section is calculated for (1) $-0.9 < \cos\theta^* < 0.9$ and (2) $-0.9 < \cos\theta^* < 0.7$. The last column gives the standard model predictions obtained from ZFITTER for $q\bar{q}$, $\mu^+\mu^-$ and $\tau^+\tau^-$, and BHWIDE for e^+e^-.

$\sqrt{s'/s}$ cut	E_{cm} (GeV)	Event type	σ (pb)	S.M. (pb)
0.1	204.9	$q\bar{q}$	$79.52 \pm 1.08 \pm 0.67$	78.87
		$\mu^+\mu^-$	$5.75 \pm 0.35 \pm 0.12$	5.98
		$\tau^+\tau^-$	$5.97 \pm 0.40 \pm 0.10$	5.98
	206.7	$q\bar{q}$	$76.40 \pm 0.83 \pm 0.64$	77.63
		$\mu^+\mu^-$	$6.16 \pm 0.28 \pm 0.12$	5.86
		$\tau^+\tau^-$	$5.97 \pm 0.30 \pm 0.10$	5.86
0.9	204.9	$q\bar{q}$	$16.03 \pm 0.48 \pm 0.21$	15.73
		$\mu^+\mu^-$	$1.74 \pm 0.16 \pm 0.01$	2.24
		$\tau^+\tau^-$	$2.16 \pm 0.25 \pm 0.04$	2.32
		$e^+e^-(1\ )$	$75.33 \pm 1.20 \pm 0.90$	74.36
		$e^+e^-(2\ )$	$14.73 \pm 0.50 \pm 0.21$	15.19
	206.7	$q\bar{q}$	$15.34 \pm 0.35 \pm 0.19$	15.38
		$\mu^+\mu^-$	$2.34 \pm 0.14 \pm 0.01$	2.19
		$\tau^+\tau^-$	$1.98 \pm 0.18 \pm 0.04$	2.27
		$e^+e^-(1\ )$	$73.40 \pm 0.91 \pm 0.70$	74.50
		$e^+e^-(2\ )$	$14.91 \pm 0.38 \pm 0.20$	15.26

Table 4: Lepton forward-backward asymmetries with statistical and systematic errors, determined for $\sqrt{s'/s} > 0.9$ and $|\cos\theta| < 0.95$. The last column gives the ZFITTER prediction.

E_{cm} (GeV)	Channel	A_{FB}	S.M.
204.9	$\mu^+\mu^-$	$0.561 \pm 0.068 \pm 0.011$	0.543
	$\tau^+\tau^-$	$0.584 \pm 0.08 \pm 0.043$	0.543
206.7	$\mu^+\mu^-$	$0.578 \pm 0.046 \pm 0.012$	0.542
	$\tau^+\tau^-$	$0.574 \pm 0.06 \pm 0.046$	0.543

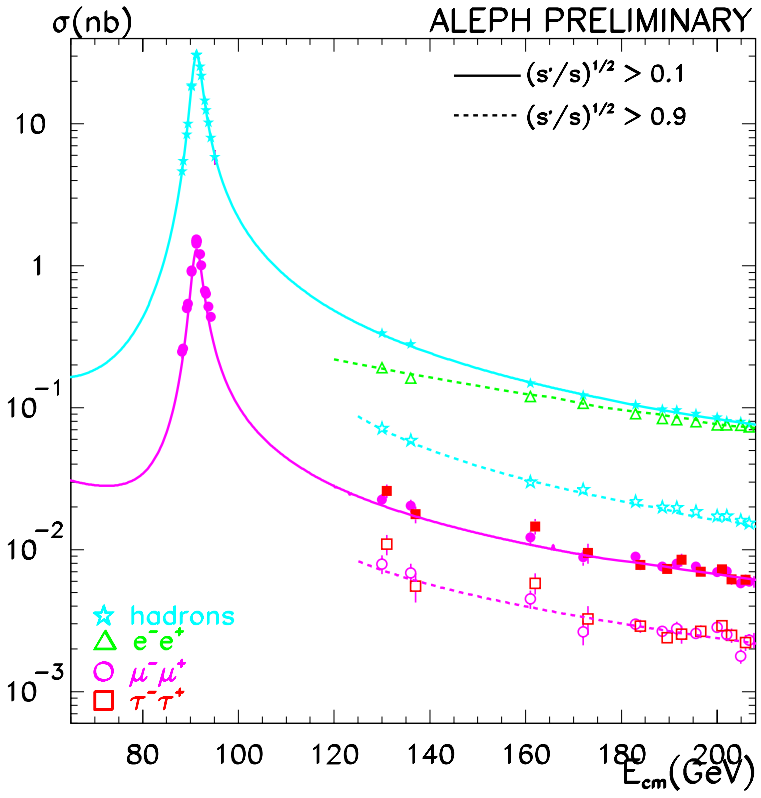

Figure 1: Cross section measurements for fermion pair production versus centre-of-mass energy. The curves indicate the expected cross-sections from BHWIDE for the Bhabha process and from ZFITTER for the other channels.

cross sections are given in a numerical form in Table 5 and are displayed in Fig. 3 for the centre of mass energy of 206.7 GeV.

2.2 Measurements of R_b, $A_{FB}^{b,c}$ and Q_{FB}^{udsc}

The ratio $R_b = \sigma_{b\bar{b}}/\sigma_{q\bar{q}}$ was determined at centre of mass energies in the range 192 to 202 GeV. Following the method described in detail in Ref. [1], the $b\bar{b}$ events were selected from the exclusive hadronic event sample by profiting from the long lifetime of b hadrons. After clustering each event into two jets, an acceptance cut requiring both jets within $|\cos\theta| < 0.9$ ensured that event vertices are well reconstructed in the vertex detector. The $b\bar{b}$ events were then tagged using the 3-dimensional impact parameter significances of tracks in the event, with which a confidence level that all tracks originate from the primary vertex is calculated [7]. The final selection cut was optimized to maximize $S_{exp}/\sqrt{B_{exp}}$, where S_{exp} and B_{exp} are the expected signal and background.

Measurements at 192 and 196 GeV (resp. 200 and 202 GeV) are combined to an averaged value at 194.5 GeV (resp. 200.2 GeV) and are given in Table 6. The evolution of R_b as a function of the centre of mass energy is compared with SM expectations in Fig. 4.

Table 5: Differential cross-sections for $\mu^+\mu^-$ and $\tau^+\tau^-$ pair production for $\sqrt{s'/s} > 0.85$. The uncertainties include statistical and systematic effects combined.

$\mu^+\mu^-$		
cosθ	$d\sigma/dcos\theta$(pb)	
	204.9 GeV	206.7 GeV
[-0.95,-0.80]	0.42 ± 0.20	0.51 ± 0.18
[-0.80,-0.60]	0.29 ± 0.15	0.43 ± 0.14
[-0.60,-0.40]	0.17 ± 0.13	0.25 ± 0.11
[-0.40,-0.20]	0.56 ± 0.31	1.00 ± 0.21
[-0.20, 0.00]	0.94 ± 0.25	0.60 ± 0.16
[0.00, 0.20]	1.00 ± 0.27	1.06 ± 0.21
[0.20, 0.40]	1.17 ± 0.29	1.61 ± 0.26
[0.40, 0.60]	1.64 ± 0.34	1.94 ± 0.28
[0.60, 0.80]	1.65 ± 0.35	2.84 ± 0.35
[0.80, 0.95]	2.33 ± 0.48	2.95 ± 0.42
$\tau^+\tau^-$		
cosθ	$d\sigma/dcos\theta$(pb)	
	204.9 GeV	206.7 GeV
[-0.95,-0.80]	0.65 ± 0.46	0.35 ± 0.27
[-0.80,-0.60]	0.50 ± 0.28	0.38 ± 0.21
[-0.60,-0.40]	0.39 ± 0.27	0.38 ± 0.21
[-0.40,-0.20]	0.21 ± 0.23	0.60 ± 0.25
[-0.20, 0.00]	0.20 ± 0.25	0.37 ± 0.20
[0.00, 0.20]	1.14 ± 0.41	1.37 ± 0.34
[0.20, 0.40]	1.73 ± 0.50	1.27 ± 0.34
[0.40, 0.60]	1.43 ± 0.48	1.35 ± 0.35
[0.60, 0.80]	1.60 ± 0.52	1.85 ± 0.41
[0.80, 0.95]	3.09 ± 1.08	2.67 ± 0.72

Table 6: Cross-section ratio and forward-backward asymmetry for b quarks for $\sqrt{s'/s} > 0.9$ and $|\cos\theta| < 0.95$. The data recorded at 192 and 196 GeV (resp. 200 and 202 GeV) are merged and appear at 194.5 GeV (resp. 200.2 GeV).

.

	194.5 GeV	200.2 GeV
R_b	$0.134 \pm 0.015 \pm 0.005$	$0.155 \pm 0.016 \pm 0.005$
$(R_b)_{SM}$	0.165	0.164
A^b_{FB}	$0.318 \pm 0.213 \pm 0.010$	$0.508 \pm 0.192 \pm 0.012$
$(A^b_{FB})_{SM}$	0.573	0.577

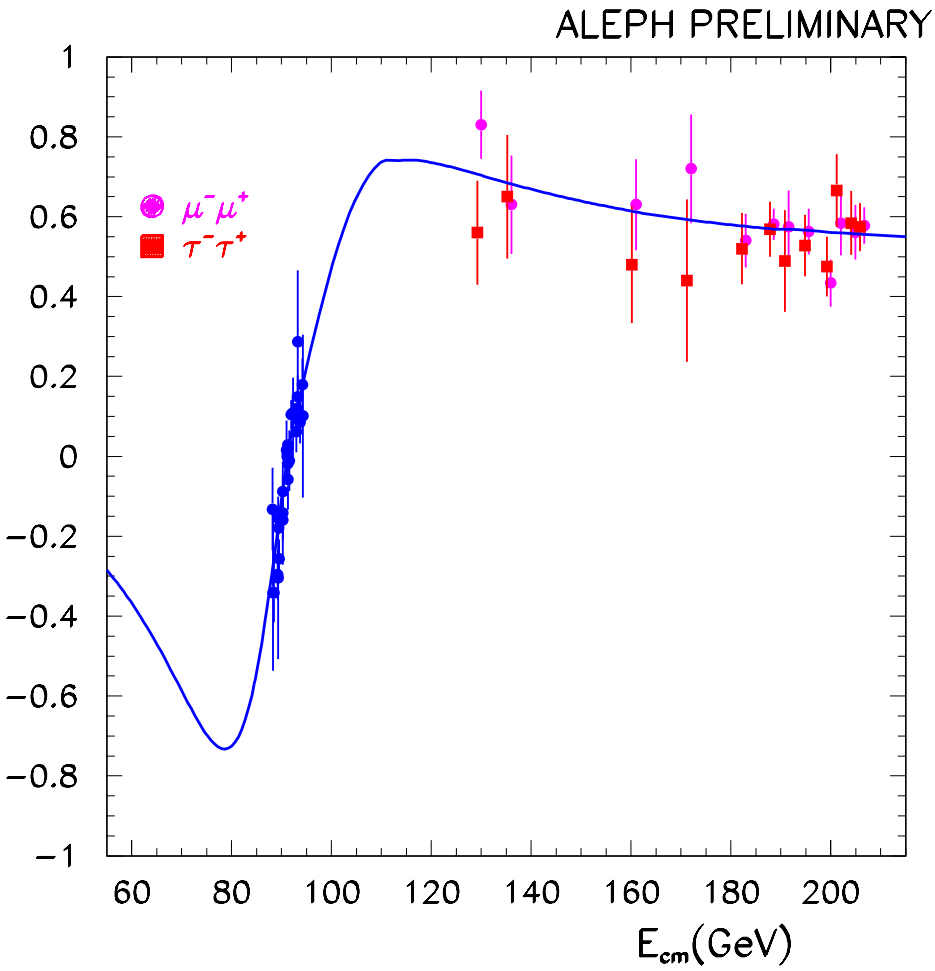

Figure 2: Asymmetry measurements for μ pair and τ pair production versus centre-of-mass energy. The curves indicate the expected asymmetries from ZFITTER.

The same b tagged events are used to measure A^b_{FB} using a jet charge technique as in [1]. Results are summarized together with the Standard Model expectations in Table 6.

On the other hand, anti-b tagged events give a measurement of the forward-backward charge asymmetry Q^{udsc}_{FB} summarized in Table 7, together with the expectation from the Standard Model in which detector effects have been taken in account.

Finally, following the analysis already mentionned in [2], an enriched $c\bar{c}$ sample is used to measure A^c_{FB} for 189 GeV. The determination of the c jet charge is obtained from a neural network combining 7 characteristic variables as in [2]. The apparent asymmetry distribution is shown in Fig. 5. The measurement is the following:

$$A^c_{FB}(|\cos\theta| < 0.9) = 0.461 \pm 0.141 \pm 0.153$$

leading to :

$$A^c_{FB} = 0.474 \pm 0.149 \pm 0.161$$

using ZFITTER[5] predictions to extrapolate from $|\cos\theta| < 0.9$ to $|\cos\theta| < 0.95$ for which an A^c_{FB} of 0.63 is expected.

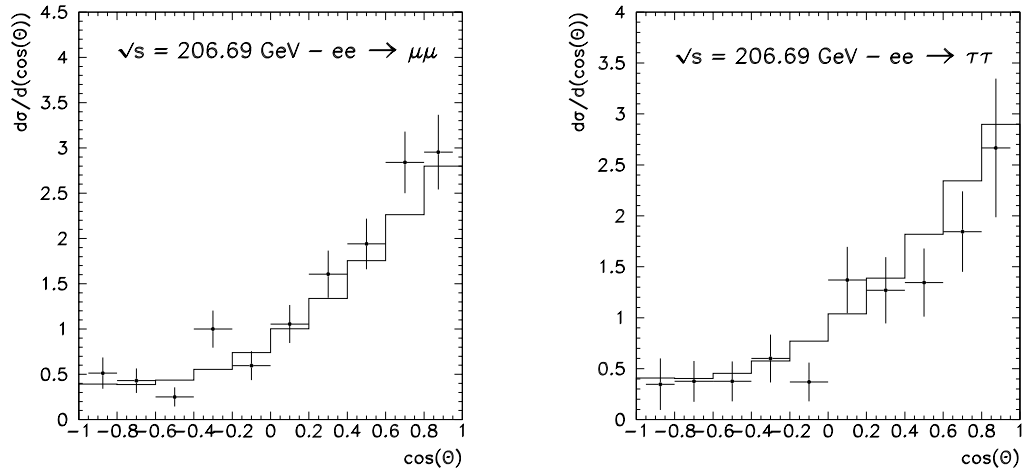

Figure 3: Differential Cross sections for lepton pair production at 206.7 GeV for $\sqrt{s'/s} > 0.85$.

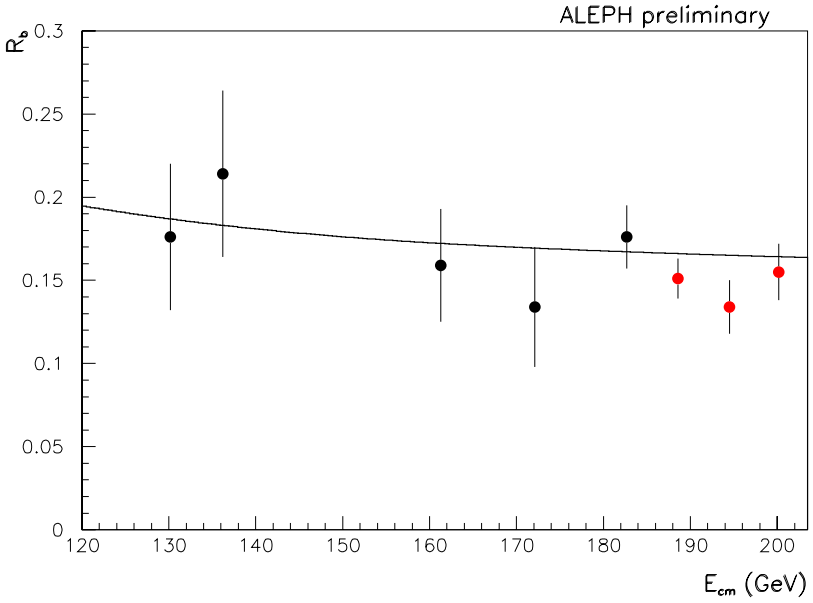

Figure 4: Measured values of R_b compared with the SM expectations

3 Interpretations in Terms of New Physics

Comparison of the measured difermion cross sections and angular distributions for $130 < \sqrt{s} < 208$ GeV with SM predictions [5] allows to place limits upon many possible extensions to the SM. The uncertainties on the theoretical predictions assumed for the comparison are 1% for the cross sections and 2% for the asymmetries. The latter error is propagated to the angular distributions. Following the method described in detail in Ref. [1], limits are given here for four-fermion contact interactions, R-parity violating

Table 7: Jet charge asymmetry measurement for u,d,s,c quarks with polar angle satisfying $|\cos\theta| < 0.9$ for data taken in the 192 to 202 GeV energy range; also given are the expectations for the measurements.

CM energy (GeV)	Q_{FB}^{udsc}	$Q_{FB}^{udsc} predictions$
192	$0.0147 \pm 0.0082 \pm 0.0013$	0.0094
196	$0.0133 \pm 0.0045 \pm 0.0014$	0.0087
200	$-0.0047 \pm 0.0051 \pm 0.0015$	0.0083
202	$0.0182 \pm 0.0069 \pm 0.0013$	0.0076

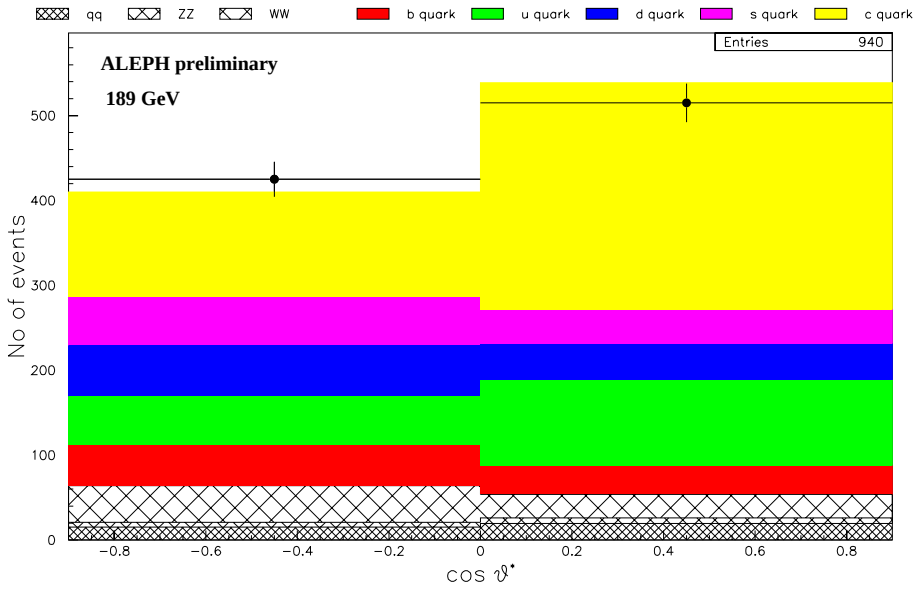

Figure 5: Distribution of the apparent asymmetry for $c\bar{c}$ selected events at 189 GeV.

sneutrinos or squarks and leptoquarks. The difermion results are also used to derive limits on TeV scale quantum gravity as described in Ref. [8].

3.1 Limits on Four-Fermion Contact Interactions

Many forms of new interactions can be parameterized by four-fermion contact interactions. These are characterized by a scale Λ, interpreted as the mass of a new heavy particle exchanged between the incoming and outgoing fermion pairs. By convention, the coupling constant is taken as $\sqrt{4\pi}$ (the mass limits scale in proportion to the assumed coupling). Following the notation of Ref. [9] contact interactions are classified according to the chirality of the initial and final state fermions. Moreover, they may depend on the fermion flavour. Fits are performed for the parameter $\epsilon = 1/\Lambda^2$. The 68% confidence level range for ϵ and the 95% confidence level lower limits on $\Lambda^{\pm}$, corresponding to constructive or destructive interference with the SM, are given in Tables 8 and 9.

Table 8: Results of contact interaction fits to leptons. The 68% confidence level range is given for $\epsilon = 1/\Lambda^2$ whilst the 95% confidence level limits are given for Λ. The results presented in the l^+l^- part of the table assume lepton universality.

Model	$[\epsilon^-,\epsilon^+]$ (TeV^{-2})	Λ^- (TeV)	Λ^+ (TeV)
$e^+e^- \to e^+e^-$			
LL	$[+0.018, +0.055]$	7.3	3.8
RR	$[+0.019, +0.057]$	7.2	3.8
VV	$[+0.009, +0.019]$	16.0	6.8
AA	$[-0.016, -0.003]$	6.9	11.7
LR	$[+0.026, +0.057]$	10.0	3.8
LL+RR	$[+0.011, +0.030]$	10.1	5.2
LR+RL	$[+0.011, +0.024]$	13.3	5.9
$e^+e^- \to \mu^+\mu^-$			
LL	$[-0.000, +0.019]$	8.6	6.3
RR	$[-0.000, +0.020]$	8.1	6.0
VV	$[+0.000, +0.007]$	14.1	10.0
AA	$[-0.002, +0.007]$	11.6	9.9
LR	$[-0.016, +0.019]$	2.3	5.8
LL+RR	$[-0.000, +0.010]$	12.0	8.6
LR+RL	$[-0.003, +0.011]$	9.7	7.9
$e^+e^- \to \tau^+\tau^-$			
LL	$[-0.044, -0.018]$	4.4	9.1
RR	$[-0.049, -0.020]$	4.1	8.8
VV	$[-0.014, -0.005]$	7.6	13.4
AA	$[-0.016, -0.004]$	7.0	12.2
LR	$[-0.214, +0.001]$	2.1	6.0
LL+RR	$[-0.022, -0.009]$	6.1	12.3
LR+RL	$[-0.016, +0.004]$	2.1	8.2
$e^+e^- \to l^+l^-$			
LL	$[-0.004, +0.011]$	8.8	7.5
RR	$[-0.004, +0.013]$	8.6	7.2
VV	$[+0.002, +0.007]$	17.7	10.7
AA	$[-0.007, -0.000]$	10.3	15.2
LR	$[+0.007, +0.024]$	10.6	6.0
LL+RR	$[-0.002, +0.006]$	12.2	10.2
LR+RL	$[+0.004, +0.013]$	15.1	8.0

Table 9: Results of contact interaction fits to quarks and quarks plus leptons. The 68% confidence level range is given for $\epsilon = 1/\Lambda^2$ whilst the 95% confidence level limits are given for Λ. The results presented in the $f\bar{f}$ part of the table assume that the contact interaction couples to all the outgoing fermion types equally.

Model	$[\epsilon^-,\epsilon^+]$ (TeV^{-2})	Λ^- (TeV)	Λ^+ (TeV)
$e^+e^- \to q\bar{q}$			
LL	$[-0.006, +0.004]$	9.3	10.2
RR	$[-0.023, -0.001]$	5.7	8.1
VV	$[-0.009, -0.001]$	9.4	14.0
AA	$[-0.003, +0.004]$	12.3	12.4
LR	$[-0.044, +0.004]$	4.3	4.3
RL	$[-0.027, -0.009]$	5.5	5.7
LL+RR	$[-0.006, +0.002]$	10.8	12.9
LR+RL	$[-0.023, -0.008]$	6.0	3.5
$e^+e^- \to f\bar{f}$			
LL	$[+0.004, +0.005]$	10.8	10.7
RR	$[-0.008, +0.005]$	8.3	9.0
VV	$[-0.001, +0.003]$	16.6	13.8
AA	$[-0.004, +0.001]$	13.1	16.6
LR	$[+0.005, +0.023]$	10.1	5.9
RL	$[-0.003, +0.012]$	9.4	7.4
LL+RR	$[-0.003, +0.003]$	13.6	13.7
LR+RL	$[+0.000, +0.009]$	13.4	9.1

3.2 Limits on R-parity Violating Sneutrinos

Supersymmetric theories with R-parity violation have terms in the Lagrangian of the form $\lambda_{ijk} L_i L_j \bar{E}_k$, where L denotes a lepton doublet superfield and $\bar{E}$ denotes a lepton singlet superfield. The parameter λ is a Yukawa coupling and i, j, k = 1, 2, 3 are generation indices. For fermion pair final states, s-channel (and to a lesser extent t-channel) exchange of an R-parity violating sneutrino can then occur. Fig. 6 shows the limits obtained using the measured differential e^+e^-, $\mu^+\mu^-$ and $\tau^+\tau^-$ cross sections. This analysis is one of very few which can probe sneutrino masses of a few hundred GeV/c^2.

3.3 Limits on Leptoquarks and R-Parity Violating Squarks

Limits on leptoquarks (LQ) are derived from all $q\bar{q}$ cross sections, asymmetries and from the charge asymmetry measurements up to 202 GeV ([1], [2], [3]). The limits are summarized in Table 10, where a leptoquark coupling of $\sqrt{4\pi\alpha_{em}}$ has been assumed. The $S_0(L)$ LQ is equivalent to a $\tilde{d}$ R-parity violating squark. By comparison, limits from the TEVATRON [11] extend to $\approx$ 225 GeV/c^2 for any leptoquark coupling strength. For first generation leptoquarks with electromagnetic coupling strength, HERA [12] excludes masses up to $\approx$ 275 GeV/c^2.

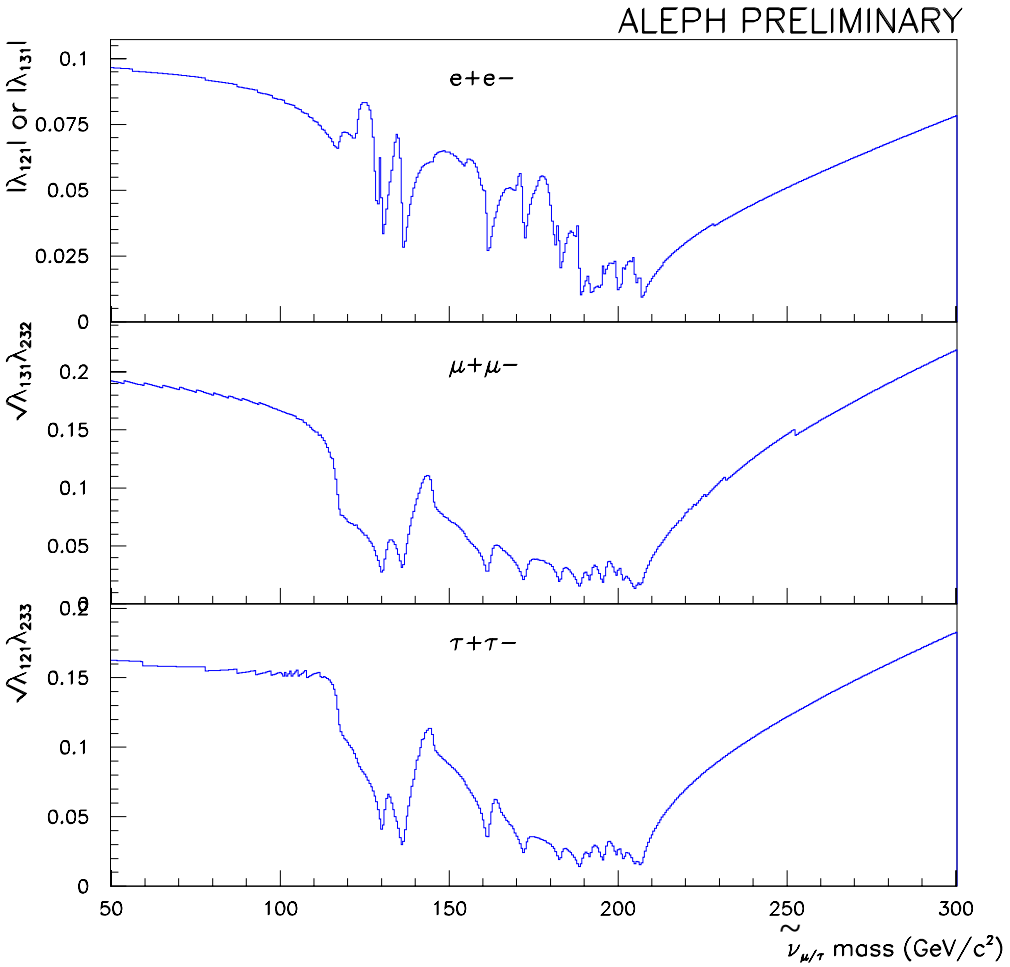

Figure 6: 95% confidence level upper limits, obtained from the lepton pair production cross sections on $|\lambda_{ijk}|$ versus the assumed $\tilde{\nu}$ mass, for $\tilde{\nu}$- couplings to a) e^+e^- b) $\mu^+\mu^-$ and c) $\tau^+\tau^-$ pairs.

Table 10: 95% confidence level lower limits on the LQ mass (GeV/c^2) for each first, second or third generation Leptoquark [10]. A dash indicates that no limit can be set and N.A denotes leptoquarks coupling only to top quarks and hence not visible at LEP.

	Limit on scalar LQ mass (GeV/c^2)						
	$S_0(L)$	$S_0(R)$	$\tilde{S}_0(R)$	$S_{\frac{1}{2}}(L)$	$S_{\frac{1}{2}}(R)$	$\tilde{S}_{\frac{1}{2}}(L)$	$S_1(L)$
LQ_{1st}	632	103	170	179	158	-	387
LQ_{2nd}	593	-	174	180	167	-	405
LQ_{3rd}	NA	NA	358	NA	-	136	747
	Limit on vector LQ mass (GeV/c^2)						
	$V_0(L)$	$V_0(R)$	$\tilde{V}_0(R)$	$V_{\frac{1}{2}}(L)$	$V_{\frac{1}{2}}(R)$	$\tilde{V}_{\frac{1}{2}}(L)$	$V_1(L)$
LQ_{1st}	829	147	409	167	340	120	620
LQ_{2nd}	846	148	408	168	314	120	633
LQ_{3rd}	448	183	NA	196	353	NA	448

3.4 Search for extra Spatial Dimensions

A solution to the hierarchy problem has been proposed in [13] where gravity is characterized by a fundamental mass scale M_D of the order ~ 1 TeV, space consists of δ extra dimensions of size R and the Newtonian gravitational constant is given by $G_N^{-1} = 8\pi R^\delta M_D^{2+\delta}$.

In this theory gravity becomes strong at distances $r \sim 1/M_D$ and measurable deviations from the SM differential cross sections for $e^+e^- \to f\bar{f}$ due to virtual graviton exchange are expected.

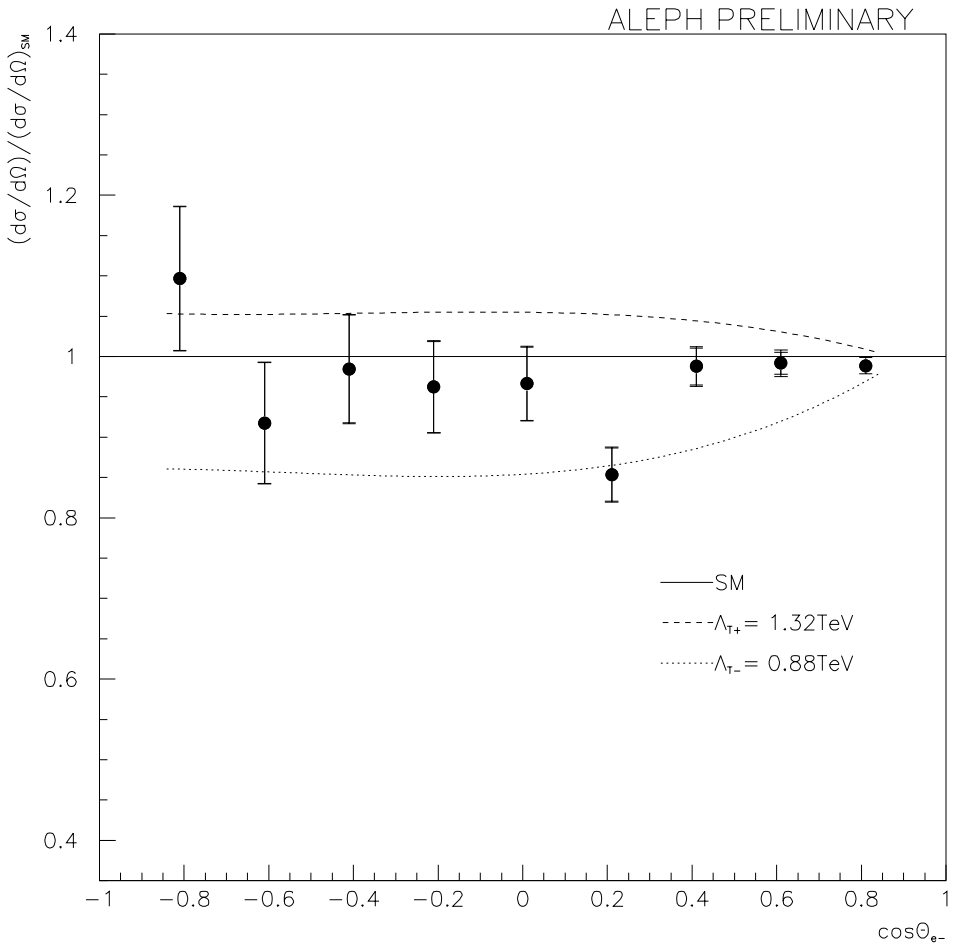

Figure 7: Measured deviation from the Standard Model as a function of the scattering angle for Bhabha cross-section, the outer error bars represent the full uncertainties dominated by the statistical error (inner error bars). Also displayed are the predicted behaviours for two cutoff energies Λ_T corresponding to the 95% CL limits.

These deviations are parametrized in terms of an ultraviolet cutoff energy Λ_T which should be of the same order of magnitude as the mass scale M_D. Details of a fit to the data to obtain lower limits on Λ_T have been given previously [8]. The fit has been repeated including the new data presented in this paper. Fig. 7 shows the measured differential cross-section for $e^+e^- \to e^+e^-$normalized to the Standard Model expectation. The prediction for graviton interactions with cutoffs given by 95% CL limits obtained from these data are indicated. In Table 11 the 68% confidence level range for $\epsilon = (1/\Lambda_T)^4$

is given as well as 95% C.L. lower limits on Λ_T^+ and Λ_T^-, corresponding to constructive and destructive interference between SM and graviton exchange amplitudes, respectively.

Table 11: Fitted values of $\epsilon = (1/\Lambda_T)^4$ and 95% confidence level lower limits on Λ_T^+ and Λ_T^-.

Channel	$\epsilon = (1/\Lambda_T)^4$ (TeV^{-4})	Λ_T^- (TeV)	Λ_T^+ (TeV)
$q\bar{q}$	$[-2.6, +3.3]$	0.67	0.65
e^+e^-	$[-1.4, -0.7]$	0.88	1.32
$\mu^+\mu^-$	$[-1.2, +1.5]$	0.79	0.77
$\tau^+\tau^-$	$[-0.9, +2.8]$	0.75	0.70
ff	$[-1.3, -0.6]$	0.91	1.32

4 Conclusions

Measurements of the hadronic and leptonic cross sections and asymmetries at the highest centre-of-mass energies reached by LEP were presented. Furthermore, measurements of R_b, A_{FB}^b and Q_{FB}^{udsc} up to 202 GeV and the measurement of A_{FB}^c at 189GeV were reported. The measurements agree with SM predictions and allow for improvements on the constraints on four-fermion contact interactions, leptoquarks, R-parity violating squarks and sneutrinos as well as TeV scale quantum gravity.

Acknowledgements

We thank our colleagues from the CERN accelerator divisions for the successful operation of LEP. We are indebted to the engineers and technicians in all our institutions for their contribution to the continuing good performance of ALEPH. Those of us from non-member states thank CERN for its hospitality.

References

[1] ALEPH Collaboration, *Study of Fermion Pair Production in e^+e^- Collisions at 130-183 GeV*, Eur. Phys. J. C12 (2000) 183.

[2] ALEPH Collaboration, *Fermion Pair Production in e^+e^- Collisions at 189 GeV and Limits on Physics beyond the Standard Model*, ALEPH 99-018 CONF 99-013. Contribution to the International Europhysics Conference on High Energy Physics, EPS-HEP99, Tampere, Finland, July 1999, Abstract #6-694.

[3] ALEPH Collaboration, *Fermion Pair Production in e^+e^- Collisions from 192 to 202 GeV and Limits on Physics beyond the Standard Model*, CONF 2000-030. Contribution to the ICHEP Conference on High Energy Physics, Osaka, Japan, July 2000, Abstract #654.

[4] S. Jadach, B. Ward, Z. Was CERN-TH 00-087 (2000)

[5] D. Bardin et al., preprint DESY 99-070 (1999), `hep-ph/9908433`.

[6] S. Jadach, W. Placzek and B.F.L. Ward, Phys. Lett. B390 (1997) 298.

[7] ALEPH Collab., *"A measurement of R_b using a lifetime-mass tag"*, Phys. Lett. B401 (1997) 150.

[8] ALEPH Collab., *"Search for extra spatial dimensions and TeV scale quantum gravity at LEP"*, ALEPH 99-051 CONF 99-027. Contribution to the International Europhysics Conference on High Energy Physics, EPS-HEP99, Tampere, Finland, July 1999, Abstract #6-417.

[9] H. Kroha, Phys. Rev. D46 (1992) 58.

[10] W. Buchmuller, R, Ruckl and D. Wyler Phys.Lett. B191 (1991) 442 ;

[11] D0 Collab., B. Abbott et al., Phys.Rev.Lett.80 (1998) 2051 ; CDF Collab., F. Abe et al., Phys.Rev.Lett.79 (1997) 4327

[12] H1 Collab., C. Adloff et al., Eur. Phys. J. C11 (1999) 447 ; ZEUS Collab., J. Breitweg et al., DESY 00-023, accepted by Eur. Phys. J.

[13] N. Arkani-Hamed, S. Dimopoulos and G. Dvali, Phys. Lett. B429 (1998) 263.